
Counterion distribution around DNA: variation with conformation and sequence

George R.Pack, Linda Wong and C.V.Prasad

Department of Biomedical Sciences, University of Illinois College of Medicine, Rockford, IL 61107, USA

Received 4 October 1985; Accepted 14 January 1986

ABSTRACT

The three-dimensional Poisson-Boltzmann equation for the distribution of counterion charge density around double helical DNA has been solved by an iterative procedure. These computations have been performed for 0.01M monovalent salt solutions. A systematic study of the ten possible sequences found among adjacent nucleotide base pairs is presented for the A, B, and C conformations of DNA. In addition, calculations of the electrostatic stabilities of these conformations of DNA allows for comparison of the charge accumulation around each of the three conformers.

INTRODUCTION

The properties of DNA, particularly its specific interactions with cellular proteins, are related to its conformational state. The interconversion between conformations can be induced by changes in the solution environment of the DNA. Perhaps the most physiologically relevant modifications of the solution environment in this context are variations in the ionic strength. The ease with which specific conformational transitions can be accomplished depends on the specific nucleotide sequences involved. As a first step toward understanding these interconversions, we have computed the approximate three-dimensional distribution of electrolyte charge density around models of DNA in the A, B, and C conformations. Calculations of the electrostatic stabilization energy for each conformer and its ten possible variations in nearest neighbor nucleotide base sequences are presented. All calculations presented here are done at a bulk electrolyte concentration of 0.01M monovalent salt.

METHODS

The distribution of electrolyte charge around the polyelectrolytic polymer, DNA, was calculated by methods developed in this laboratory and described in detail previously (1-3). The equations solved invoke a dielectric continuum model and utilize the "mean field approximation" in which the potential

of mean force is replaced by the mean potential (4), making the results equivalent to a numerical solution of the three dimensional Poisson-Boltzmann equation. These calculations use the spatial coordinates, as determined by x-ray diffraction studies, of each atom of a thirty base-pair sequence. The atomic positions used were those obtained by Fuller *et al* (5) for the A-conformer, those of Arnott and Hukins (6) for the B-conformer, and those of Marvin *et al* (7) for the C-conformer. A partial atomic charge calculated from molecular orbital theory is associated with each atomic center in such a way that each nucleotide has a total charge of one electron (8). These charges give rise to an anisotropic potential in the volume surrounding the DNA. The magnitude of the potential, Ψ_i , at a point, i , in the environment of DNA is calculated according to equation (1):

$$(1) \quad \Psi_i = \sum_j^{\text{DNA}} Q_j / D r_{ij} + \sum_{k \neq i}^{\text{Env}} q_k / D r_{ik}$$

in which Q_j represents the charge on the j 'th atom of DNA; q_k represents the average charge at a point, k , in the environment; and D is the bulk dielectric constant of water. To adequately represent the spatial variations in the potential, a grid composed of a large number of points was constructed to contour the surface of DNA. The method by which this is done is described here. The volume around the DNA was partitioned such that each point could be associated with the midpoint of one finite element of volume, V_i . The average charge in each volume element could then be calculated and assigned to the point, i , by equation (2):

$$(2) \quad q_i = V_i N e [\exp(-e\Psi_i/kT) - \exp(e\Psi_i/kT)]$$

where N is the number density of positive (and negative) electrolyte ions in bulk solution; e is the electronic charge; T is the absolute temperature; and k is the Boltzmann constant. The calculations are done by successive application of equations (1) and (2) and are considered complete when there is little numerical difference (less than 1 part in 10,000) between the results of two successive iterations. Approximately 40 to 50 iterations, each consuming about 10-15 minutes of CPU time on an Amdahl 5860 computer, were required for each of the eighteen calculations presented. All calculations were performed in double precision (64-bit words).

The division of the volume surrounding DNA into numerous elements was accomplished by defining "repeat units" of two nucleotide pairs each, as the symmetry unit for the DNA. The thirty-base-pair segment was constructed by the standard transformations. The repeat distance along the helical axis was

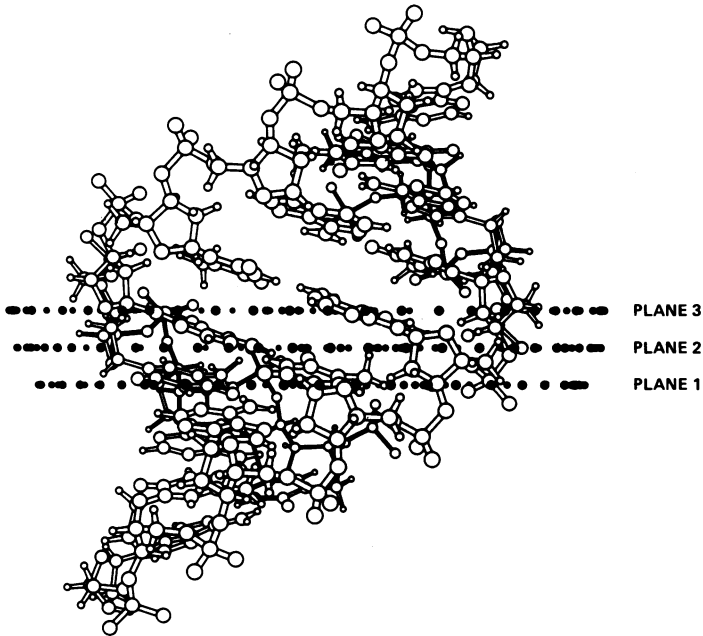


Figure 1 The innermost layer of the three unique planes of volume elements perpendicular to the helical axis of the A-conformer of DNA. One "repeat unit" of the environment is shown along with four "repeat units" (eight base pairs) of DNA. At least one atom of each of these DNA repeats was required for the contouring of the environmental shroud.

5.12 $\overset{\circ}{\text{Å}}$ for the A-conformer, 6.76 $\overset{\circ}{\text{Å}}$ for B, and 6.64 $\overset{\circ}{\text{Å}}$ for C, with angular displacements of 65.4°, 72°, and 78°, respectively. Planes perpendicular to the helical axis and points beyond the contours of the van der Waals' surface of the DNA were defined by a rolling sphere algorithm. Three planes were defined for the A-form and repeat unit and 4 planes were defined for the B- and C-forms. The distances between planes were 1.71 $\overset{\circ}{\text{Å}}$, 1.69 $\overset{\circ}{\text{Å}}$, and 1.66 $\overset{\circ}{\text{Å}}$, respectively for the A-, B-, and C-forms. By "rolling" a sphere of diameter equal to the interplanar separation in each of the planes, a closed curve was defined by the trace of the midpoint of the sphere for each plane. Points were placed along this curve at intervals approximately equal to the interplanar spacing. Layers of points beyond this innermost curve were then defined analogously, considering the previous inner curves to be part of the DNA. The points in the innermost layer were set at about 0.85 $\overset{\circ}{\text{Å}}$ from the van der Waals' surface. In this way, successive layers of points were constructed to fill the space

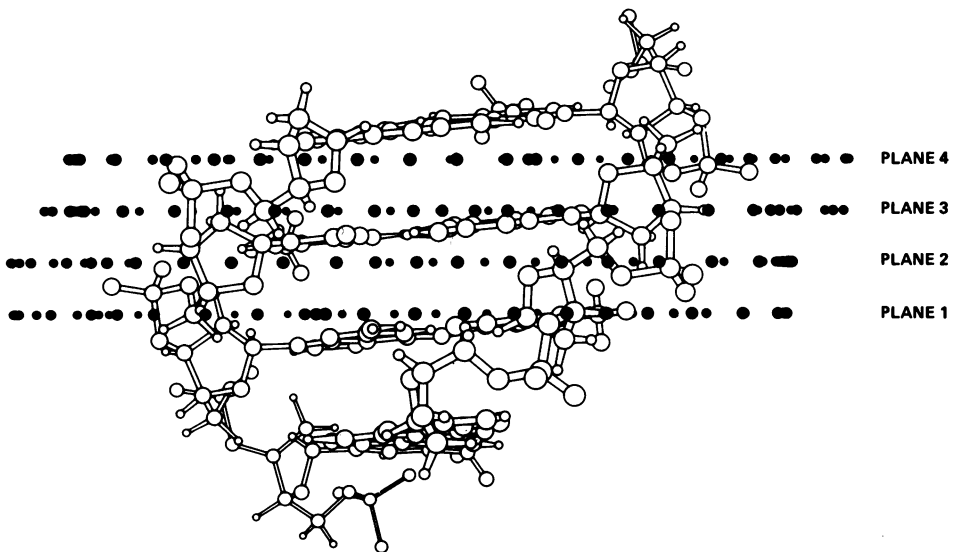


Figure 2 The innermost layer of the four unique planes of volume elements perpendicular to the helical axis of the B-conformer of DNA. Two repeat units of DNA are shown.

increasingly farther radially from the DNA surface. The spacing between planes was set as the diameter of the rolling sphere. Each point is considered to be the center of a finite element with a volume approximately equal to the cube of the interplanar spacing.

Figures 1, 2, and 3 depict the locations of the innermost layers of points for the A-, B-, and C-forms, respectively. For ease of discussion, regions in which the points are placed at a particular uniform density are named "shrouds." The innermost shrouds have the highest density of points. The calculations for the A-conformer used an innermost shroud of 3 planes with 6 layers of volume elements adjoined to an intermediate shroud of 2 planes with 4 layers of volume elements and an outer shroud of one plane with 5 layers of points. Each set of shrouds was set up for each adjacent repeating unit. The volume elements enlarge with each successive shroud in order to span the repeat unit distance. The B- and C- conformers each used repeat unit shrouds of 4 planes with 6 layers adjacent to one of 2 planes with 5 layers and then one of 1 plane with 6 layers. The calculations, therefore, encompassed the volume within about 60Å of the DNA surface for each conformation. The calculations are done by solving equations (1) and (2) for all points in the central repeat unit. This defines a set of environmental charges that are

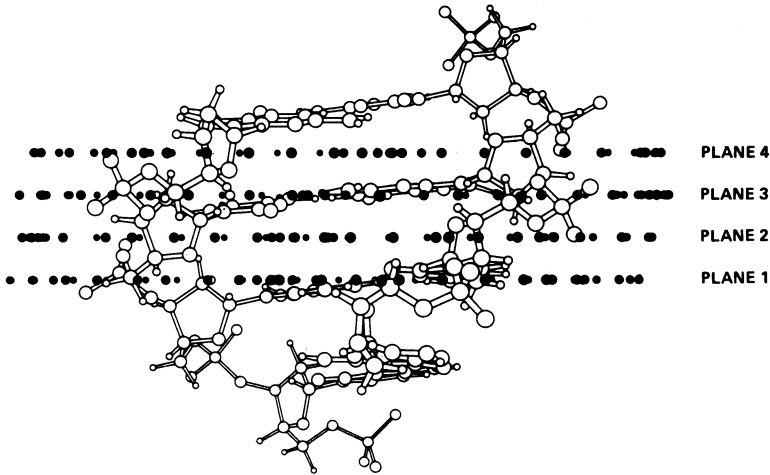


Figure 3 The innermost layer of the four unique planes of volume elements perpendicular to the helical axis of the C-conformer of DNA. Two repeat units of DNA are shown.

assumed to be equal in the remaining 14 identical repeats. The summations in equation (1) include all points in the 15 repeats.

There are several significant approximations in the model used for these calculations. Perhaps the most important is that water molecules are not explicitly considered. The effect of this approximation is difficult to assess. If waters of hydration are bound tightly to the surface of DNA they might impede the access of the counterions to restricted regions, such as the grooves, particularly at low ionic strengths. A second approximation is that the DNA has a static structure with non-varying contours represented by the x-ray diffraction results. Related to this is the assumption that a conformation has an invariant backbone structure regardless of nucleotide base sequence. A further approximation, that the ions can be represented by point charges, has been evaluated previously (3) and shown to yield results that are qualitatively very similar to the present calculations. While these approximations must be considered in evaluating the quantitative precision of the results, the qualitative results are expected to be quite reliable.

RESULTS AND DISCUSSION

Figures 4 and 5 present a pictorial representation of the variation of electrolyte charge density in the region spanned by the first six layers of volume elements in the three planes of a repeat unit around the A conformation of DNA. The most striking feature of these cross-sectional views is the great

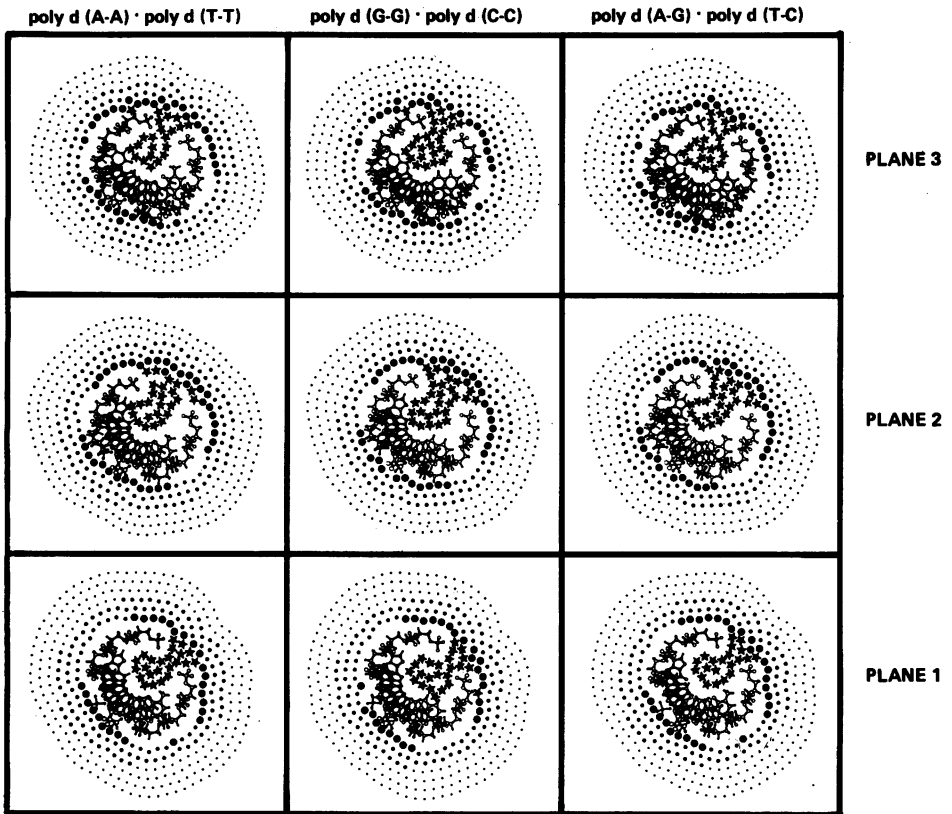


Figure 4 Illustration of the environmental charge density in the vicinity of the three purine (3'-5') pyrimidine homopolymer sequences in the A conformation in .01M monovalent salt. The three planes correspond to those in Figure 1, rotated by 90°. The stars represent volume elements in which the local concentration is greater than 3M. The large circles correspond to concentrations greater than 1M but less than 3M. The intermediate circles represent concentrations greater than .1M, while the small circles correspond to concentrations, in this inner shroud, that are greater than .01M. The volume displayed extends 10.24A from the van der Waals' surface of the DNA molecule, shows slight variations on the sequence and is much different than the volumes displayed in Figures 6-9.

accumulation of charge density that is present in the deep major groove for all of the sequences considered. Opposite the major groove, there is another region of counterion charge accumulation along the flat surface corresponding to the minor groove. The topography of the surface, however, clearly dictates that the region of highest charge accumulation be in the major groove. Each

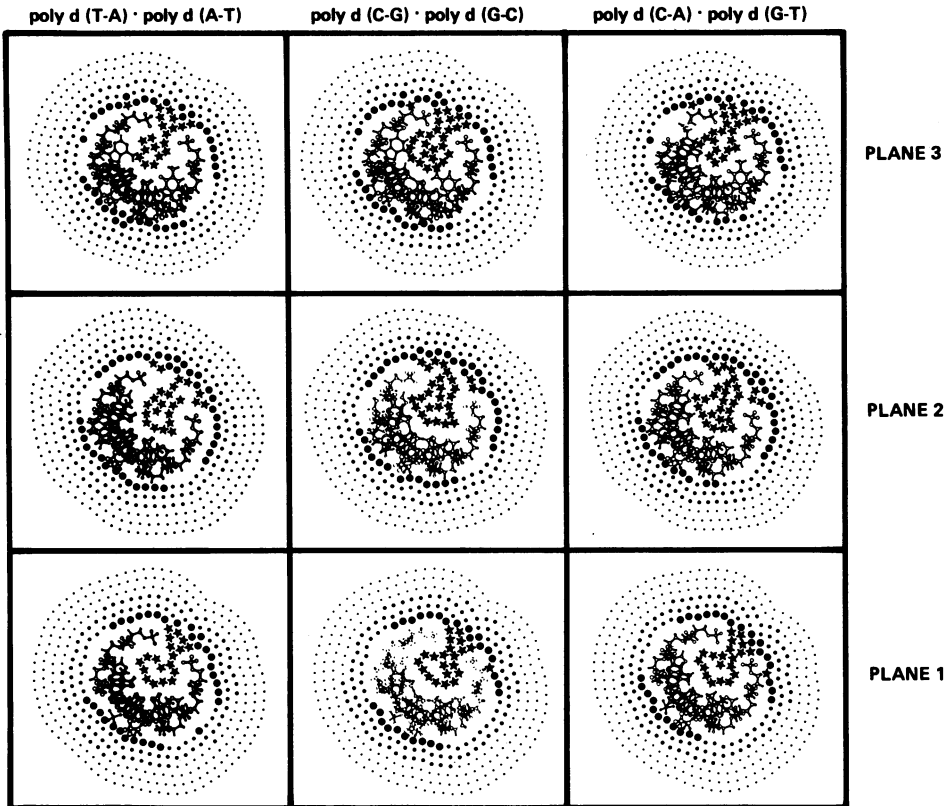


Figure 5 The environmental charge density around the three alternating purine-pyrimidine heteropolymers in the A conformation. See legend to Figure 4.

sequence shows considerable variations in counterion accumulation along the helical axis. Plane one (Figure 1) consistently has the lowest electrolyte concentration and plane two has the highest. The fact that this trend holds for the homopolymers poly d(A-A)·poly d(T-T) and poly d(G-G)·poly d(C-C) indicates that the variation is not due to attraction for particular bases, but that it is a structural property of the sugar-phosphate backbone in the A conformation.

Figures 6 and 7 show the regions of counterion accumulation around the various sequences of the B-conformer. This conformer is longer and narrower than the A-form, having a less pronounced major groove (near the bottom of each frame) and having a true minor groove into which ions can penetrate. The

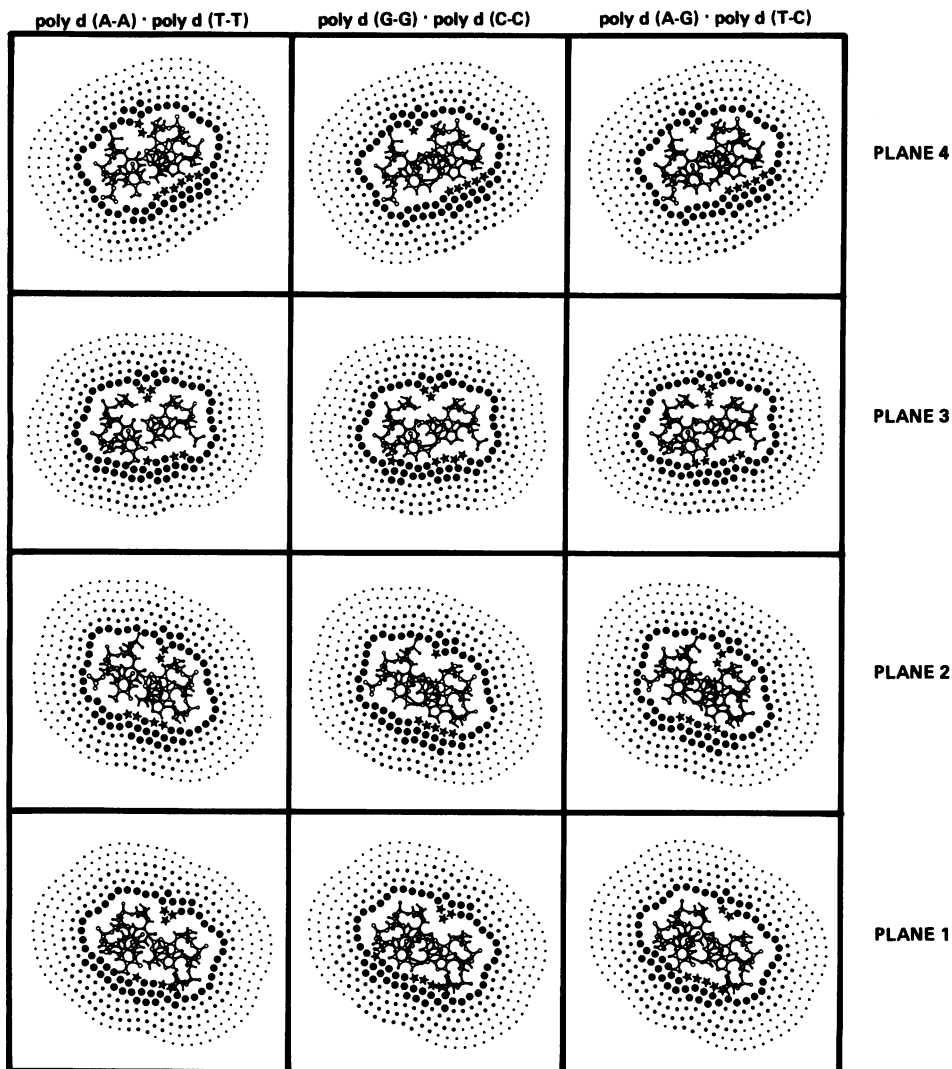


Figure 6 The environmental charge density around the three homopolymer duplexes in the B conformation. See legend to Figure 4. The volume displayed extends 10.14Å from the van der Waals' surface of DNA.

incursions into the minor groove can be seen to rotate counter-clockwise from planes one through four, following the rise of the right-handed helix. Since there is less groove volume to be occupied than in the A-form, there is a more uniform distribution of ions around the surface of the B-conformer. Four

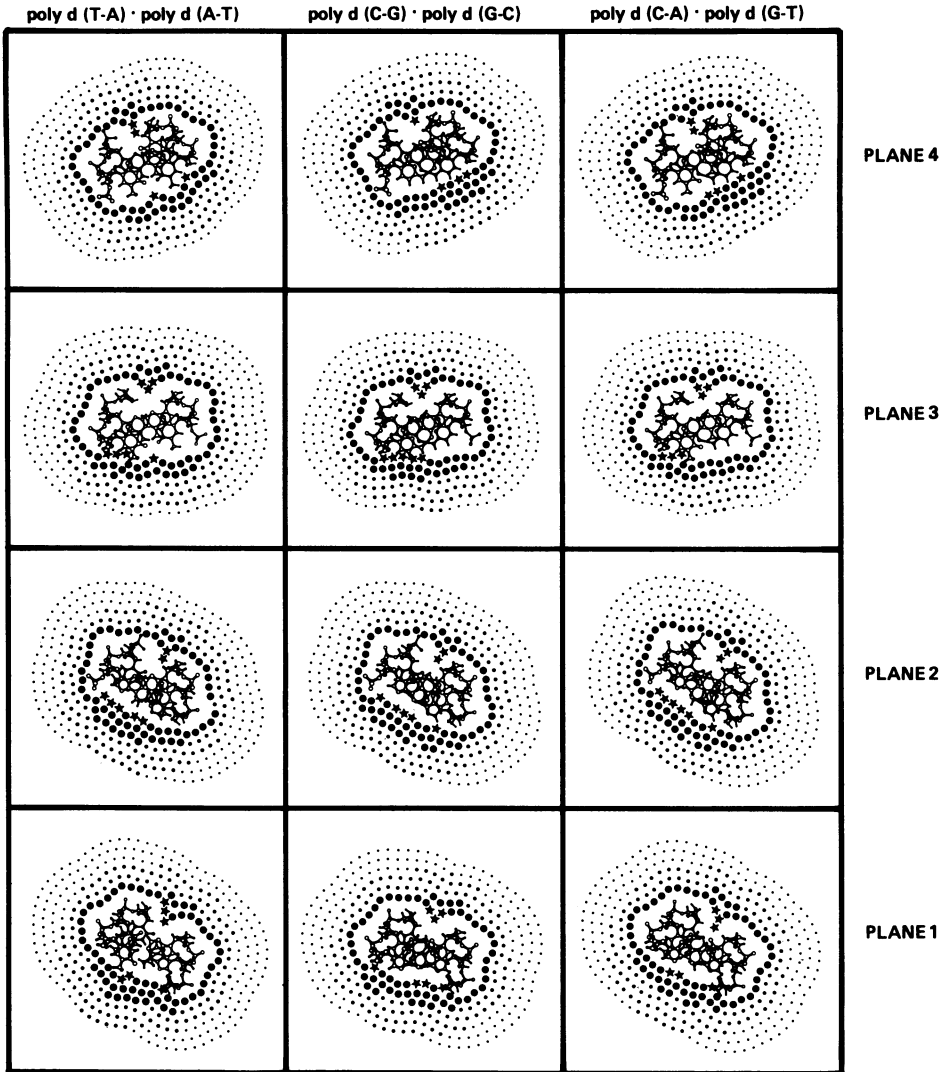


Figure 7 The environmental charge density around the three alternating purine-pyrimidine heteropolymers in the B conformation. See legend to Figure 4.

planes were set up for each repeat unit to maintain approximately the same interplanar spacing for all conformers. The volume spanned by the six planes depicted in Figures 6 and 7 extends 10.14Å from the DNA van der Waals' surface. The volume spanned by each plane represented in Figures 4 and 5 for the

A-conformer is about 1950\AA^3 , the volume of each plane around the B-conformer (Figures 6 and 7) is about 1650\AA^3 . The average counterion concentration is clearly significantly greater at the surface of the A-conformer than at the surface of the B-conformer. This is a result of the very large accumulation in the major groove of the A-form. We note that the concentrations at that part of the surface not near the grooves are, in fact, larger around the B-form than around the A-form.

The C conformation of DNA was first observed as the low humidity form of the lithium salt of DNA. It has been shown to be quite similar to the B conformation (9) and it has been suggested (10) that there may be a continuity of forms spanning the B and C families. More recent studies (11) have suggested that the C to B conformational transition of the sodium salt of DNA passes through an intermediate A-form. Since it seems likely that the C-form may play some significant physiological role, we have included calculations on this conformer. The results of these calculations, depicted in Figures 8 and 9, show clear similarities of the C-form to both the A-and the B-forms. While the helical parameters are very similar to those of the B-form, these cross-sectional views show a very deep and wide minor groove somewhat resembling the major groove of the A-form. The average counterion charge density is very similar to that found around the B-form. Presumably, this stems from the similar helical parameters giving rise to similar average anionic charge densities between the B and C double helices. While the angular distribution of counterion charge is fairly uniform around the C-form, as it is around B-, and unlike that around A-, the small amount of charge density associated with the major groove of the C-form is obvious from Figures 8 and 9.

ENERGETICS

The occurrence of a particular conformation of DNA depends upon the free energy of the entire system of charges. The expression for the free energy of a system described by the Poisson-Boltzmann equation can be derived by a formal charging process in which the charges of the macroion and those of the electrolyte ions are varied from zero to their full charge. During this (formal) process the electrolyte ion distribution changes. Oosawa has shown, by this procedure, that the free energy of the equilibrium distribution described by the Poisson-Boltzmann equation is given by: (12)

$$G = \sum_i \sum_j Q_i Q_j / Dr_{ij} + \sum_k \sum_l Q_k q_l / Dr_{kl} + 1/2 \sum_{k \neq l} q_k q_l / Dr_{kl} + kT \sum_k q_k^+ \ln (q_k^+ / q_k^0) V_k$$

in which q_k^+ is the amount of cationic charge in volume element V_k , and

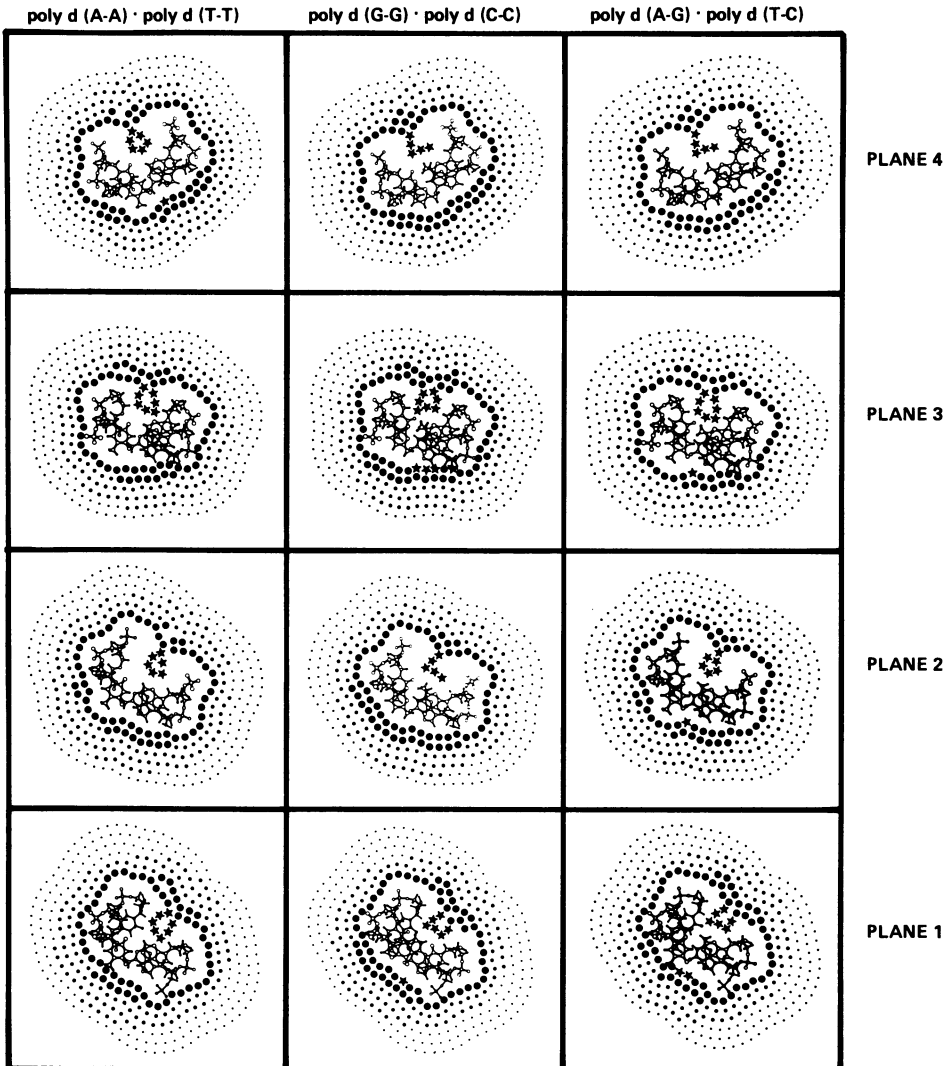


Figure 8 The environmental charge density around the three homopolymer duplexes in the C conformation. See legend to Figure 4. The volume displayed extends 9.96Å from the van der Waals' surface of DNA.

q_k^0/V_k is the bulk counterion charge density (molarity).

The individual terms on the right hand side of the free energy expression have straightforward physical interpretations. The first term is the electrostatic energy of the isolated, charged DNA; the second term is the

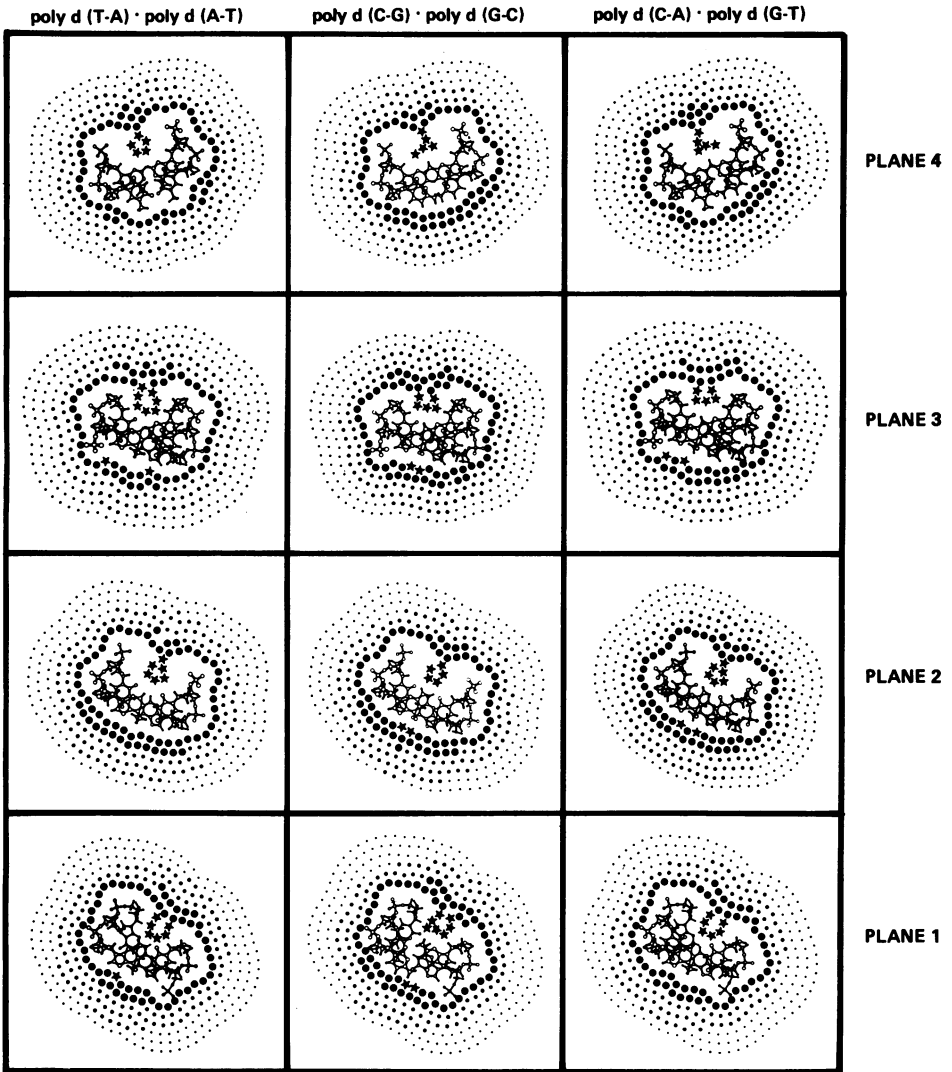


Figure 9 The environmental charge density around the three alternating purine-pyrimidine heteropolymers in the C conformation. See legend to Figure 4.

electrostatic energy of the DNA-environment interaction (the "electrostatic phosphate screening"); the third is the internal electrostatic energy of the structured counterion charge distribution; the final term is the entropy associated with the distribution of counterions.

The advantage of using this expression for the free energy over previous

TABLE I

Contributions to the variable electrostatic free energy. The stabilization due to "phosphate screening", G_{es}^{ps} , the destabilization due to the "environmental self-energy", G_{es}^{ese} , and the G_{es}^{eg} contribution of entropy, TS , are shown in units of kcal/mol of repeating unit, (4 nucleotides). All conformations in .01M monovalent salt.

$$G_{es}^{ps} = \sum_i \sum_k Q_i q_k / Dr_{ik} ; G_{es}^{ese} = 1/2 \sum_{k \neq l} q_k q_l / Dr_{kl} ; TS = kT \sum_k q_k^+ \ln (q_k^+ / q_k^0) v_k$$

Conformation	Sequence	G_{es}^{ps}	G_{es}^{ese}	-TS	G
A	poly d(C-G)•poly d(G-C)	- 40.91	29.59	+ 2.97	- 8.35
	poly d(G-G)•poly d(C-C)	- 40.03	29.70	+ 2.97	- 8.36
	poly d(A-A)•poly d(T-T)	- 40.82	29.50	+ 2.98	- 8.34
	poly d(C-A)•poly d(G-T)	- 40.87	29.54	+ 2.99	- 8.34
	poly d(A-G)•poly d(T-C)	- 40.91	20.58	+ 2.97	- 8.36
	poly d(T-A)•poly d(A-T)	- 40.44	29.12	+ 3.00	- 8.32
B	poly d(C-G)•poly d(G-C)	- 32.89	23.86	+ 2.37	- 6.66
	poly d(G-G)•poly d(C-C)	- 32.84	23.81	+ 2.36	- 6.67
	poly d(A-A)•poly d(T-T)	- 32.89	23.82	+ 2.38	- 6.69
	poly d(C-A)•poly d(G-T)	- 32.93	23.85	+ 2.38	- 6.66
	poly d(A-G)•poly d(T-C)	- 32.89	23.82	+ 2.37	- 6.70
	poly d(A-T)•poly d(T-A)	- 32.88	23.81	+ 2.39	- 6.68
C	poly d(C-G)•poly d(G-C)	- 33.49	24.25	+ 2.58	- 6.66
	poly d(G-G)•poly d(C-C)	- 33.50	24.25	+ 2.57	- 6.68
	poly d(A-A)•poly d(T-T)	- 33.58	24.30	+ 2.60	- 6.68
	poly d(C-A)•poly d(G-T)	- 33.51	24.25	+ 2.59	- 6.67
	poly d(A-G)•poly d(T-C)	- 33.53	24.27	+ 2.58	- 6.68
	poly d(A-T)•poly d(T-A)	- 33.55	24.27	+ 2.59	- 6.69

calculations is that the full effect of assembling the structured ion atmosphere is formally considered. Calculations in which the free energy is represented by a pairwise summation of anion-anion potentials of mean force, in principle, also consider the full electrostatic energy and the entropic form. These potentials of mean force may be obtained from the analytic solution of the linearized Poisson-Boltzmann equation, computer simulations of ionic solutions by Monte Carlo or Molecular Dynamics methods, or by other statistical mechanical approximations to anion-anion interactions in solution. The principle shortcoming of their use, however, resides in the transferal of free solution-derived potentials of mean force to the "internal" interactions between charged groups within a macroion. It is difficult to estimate the magnitude of the effect that the constraint of the macroion surface imposes on the free energy of the counterion distribution, although Figures 4-9 illustrate the effect on the counterion distribution itself.

Table I presents the results of the calculation of those terms that contribute to the variations in free energy among the ten possible sequences for each of the A, B, and C conformations of DNA. These calculations have been done for all conformations and sequences in solutions of .01M monovalent salt. The calculations utilize the full environmental charge distribution as calculated in the Poisson-Boltzmann approximation detailed above.

CONCLUSIONS

The calculated distributions of electrolyte charge show a far greater dependence on conformation than on nucleotide base sequence. The cross-sectional views of the charge density, as contoured to the nucleic acid surface, generated by the rolling sphere algorithm, reveal significant variations in the penetration into the grooves of the different conformations. The deep penetration of the sphere into the major groove of the A-conformer and into the minor groove of the C-conformer allows high concentrations to accumulate into restricted locations. This may be compared with the more diffuse distributions calculated around the B-conformer with two identifiable, yet relatively open, grooves.

The use of idealized conformations from fiber diffraction studies allowed a separation of the effects of sequence and conformations. The observed small but significant variations of DNA structure with sequence can be expected to lead to greater sequence dependence of counterion accumulation than the present calculations indicate. These observed structural variations are due, in part, to the forces that the counterions exert on the nucleic acid and may be expected to show significant dependence on the electrolyte concentration. In this way, local microheterogeneity of structure might be expected to be even more pronounced in solution than in the crystalline environment.

ACKNOWLEDGEMENTS

This work was supported by grants GM29079 and RR5369 from the National Institutes of Health and by a grant from the Medical Service Plan of UICOM-Rockford. Additional generous support from the Sundstrand Corporation is gratefully acknowledged.

REFERENCES

1. Klein, B.J. and Pack, G.R. (1983) *Biopolymers* **22**, 2331-2352.
2. Pack, G.R. (1983) *Int. J. Quant. Chem. QBS10*, 61-71.
3. Pack, G.R. and Klein, B.J. (1984) *Biopolymers*, **23**, 2801-2823.

4. Kirkwood, J.G. (1934) *J. Chem Phys.* 2, 767-781.
5. Fuller, W., Wilkins, M.H.F., Wilson, W.R. and Hamilton, L.D. (1965) *J. Mol. Biol.* 12, 60-80.
6. Arnott, S. and Hukins, D.W.L. (1972) *Biochem. Biophys. Res. Comm.* 47, 1504-1509.
7. Marvin, D.A., Spencer, M., Wilkins, M.H.F. and Hamilton, L.D. (1961) *J. Mol. Biol.* 3, 547-565.
8. Miller, K.J. (1979) *Biopolymers* 18, 959-980.
9. Arnott, S., and Selsing, E. (1975) *J. Mol. Biol.* 98, 265-269.
10. Zimmerman, S.B., and Pfeiffer, B. (1980) *J. Mol. Biol.* 142, 315-330.
11. Rhodes, N.J., Mahendrasingham, A., Pigram, W.J., Fuller, W., Brahm, J., Vergne, J. and Warren, R.A.J. (1982) *Nature*, 296, 267-269.
12. Oosawa, F. (1971) in "Polyelectrolytes" Chapter 3, (Marcel Dekker, Inc.) New York, New York.